Doppler Shift Estimation for Satellite Communications using Linear Estimators

(article starts on next page)

Doppler Shift Estimation for Satellite Communications using Linear Estimators

André B. de F. Diniz*†, Thomas Eriksson*, and Ulf Gustavsson*†

*Department of Electrical Engineering, Chalmers University of Technology, Gothenburg, Sweden

†Ericsson Research, Gothenburg, Sweden

Email: *{andredin, thomase}@chalmers.se, †ulf.gustavsson@ericsson.com

Abstract—Doppler shifts are an undesired effect that takes place in wireless signal transmission whenever there is relative movement between transmitter and receiver. In future communication generations, where low Earth orbit (LEO) satellites play a relevant role, such a phenomenon is expected to be strong with respect to satellites in higher altitudes, as LEO satellites travel at very high speeds. In this paper, we initially study this problem and propose a simple signal model to develop a standalone multi-step Doppler estimation approach based on linear estimators. Simulation results show practically unbiased estimates with variances close to the Cramer-Rao lower bound even in low signal-to-noise ratio regimes, demonstrating the potential of this technique in future non-terrestrial network systems.

Index Terms—Doppler shift, Estimation theory, Satellite communications

I. Introduction

As 5G communication systems are currently being deployed, interest in both 5G evolution and the upcoming 6G systems is large. One of the features of both 5G evolution and 6G is to guarantee continuous global connectivity, or coverage everywhere. Non-terrestrial networks will be highly relevant to meet such a requirement, especially in areas that are not easily covered by terrestrial ones [1]. To provide the required quality of service in a wide range of applications that demand high data rates, coverage and reliability, low Earth orbit (LEO) satellites are preferred in relation to geostationary satellites [1], [2]. This is due, for example, to the shorter propagation delays associated with LEO satellites and their capability to cover remote areas.

LEO satellites orbit the Earth at relatively high speeds, usually between 4-7km/s, causing very strong Doppler effects, which in turn generate carrier frequency offsets [3]. In orthogonal frequency division multiplexing (OFDM), they may cause time and frequency synchronization errors, generating inter-carrier interference [4], [5]. Doppler estimation and synchronization methods are therefore of great importance.

The Doppler synchronization problem has been studied in the literature and several techniques have been developed. In [6], two methods are developed to give frequency offset estimates: the first one uses primary synchronization signals (PSS), where the frequency offset estimation is carried out by solving a one-dimensional optimization problem through a grid search; the second one, together with PSS, explores the redundancy of the cyclic prefix in OFDM symbols to improve performance and reduce the computational complexity. For the latter, in

particular, simulations show suitability for downlink frequency synchronization.

Another method proposed in [7] utilizes turbo codes and a Gaussian process model to estimate Doppler offsets in the low signal-to-noise ratio (SNR) regime without using training sequences. Initially, the soft outputs of the turbo decoder at the receiver side are used to coarsely estimate the Doppler shift. An objective function representing the performance of the frequency offset compensation is replaced by a prediction function based on the Gaussian process model, such that the optimal frequency offset can be efficiently found using the Newton-Raphson method. Maximum likelihood estimation is used to improve the coarse estimate. It was shown that the root mean square error approaches the modified Cramer-Rao lower bound (CRLB) for $E_b/N_0 \geq 2$dB, with a computational complexity lower than that of other turbo-code based synchronization methods.

The orthogonal time-frequency space modulation is explored in [8], enabling a constant channel representation in the delay-Doppler domain rather than a varying one in the time-frequency domain [9]. In this synchronization technique, the carrier frequency offset comprises the sum of the fractional and large-scale carrier frequency offsets. For the former, the received time signal is transformed into a delay-time one and the correlation between consecutive rows is explored to give the best linear unbiased estimator. For the latter, the maximum length sequence is placed in the delay domain and the autocorrelation characteristics are exploited to produce the estimate. Results show a wider frequency offset estimation range and higher accuracy in relation to the method developed in [10], although with a slightly higher overhead.

In this paper, we conduct a study on Doppler shift estimation using known pilot signals and linear estimators. Linear estimators have the advantage of having a relatively simple implementation and predictable performance. We begin our investigation with a simple non-linear signal model, on which we apply a Taylor series expansion to get a linear estimator with a predictable worst-case estimator bias. Furthermore, we develop a standalone multi-step procedure to estimate the Doppler shift based on the mean square error (MSE) criterion. Simulations show, for an analyzed set of system requirements, that our proposed algorithm gives a close to unbiased estimate with variances approaching the CRLB for a wide range of SNR values. The proposed algorithm shows a better performance, in terms
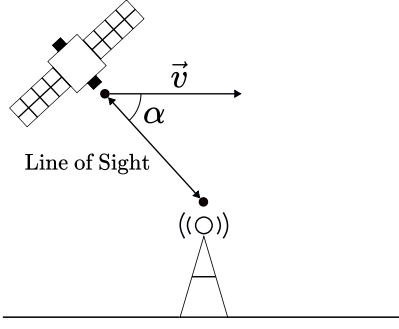
Fig. 1. Transmission scenario of a LEO satellite serving a ground terminal. Here, α is the angle between the LoS component and $\vec{v}$, the vector describing the direction and speed of the satellite.

of bias and variance, than the well-known Tretter's method for frequency estimation [11].

The paper is organized as follows. In Sec. II, we present the reference signal model and in Sec. III we discuss the procedure to estimate the parameters of interest. In Sec. IV, we show the achieved results from the proposed estimation algorithm and compare them to the ones acquired with Tretter's method. Finally, in Sec. V, we provide the conclusions from this study.

II. SIGNAL MODEL

Assuming line of sight (LoS) conditions for the transmission of a pilot signal from a LEO satellite to a ground terminal (or vice-versa), we consider the scenario illustrated in Fig. 1. We model the Doppler-shifted received signal as

$$y[n] = e^{j\varepsilon} e^{j\Omega_d\left(n - \left(\frac{L-1}{2}\right)\right)} x[n] + w[n]. \qquad (1)$$

In Eq. (1), ε denotes a constant phase term due to the distance between the satellite and the Earth device and unknown phase shifts in the hardware, Ω_d the normalized Doppler shift, $x[n]$ an all-ones vector of length L representing the pilot signal, $n = 0, \ldots, L-1$ and $w[n] \sim \mathcal{CN}(0, \sigma_w^2)$. For simplicity, we restrict L to be even, but the developed method can be easily extended to accommodate odd pilot lengths.

The normalized Doppler shift is given by $\Omega_d = 2\pi f_d/f_s$, where f_d represents the Doppler shift and f_s the sampling frequency, both given in Hz. The Doppler shift is calculated by $f_d = v f_c \cos\alpha/c$, where $v = |\vec{v}|$, as depicted in Fig. 1, given in m/s, f_c is the carrier frequency in Hz and c the speed of light in m/s. We introduce the normalized Doppler shift with the largest value Ω_W, for which α has the smallest analyzed angle. In our study, we consider the worst case situation where the satellite is at the horizon, so $\alpha = 0$ and $\Omega_W = 2\pi v f_c/(cf_s)$.

III. ESTIMATION PROCEDURE

To estimate ε and Ω_d, we apply a multi-step approach. Based on the found estimates, we compensate the received signal $y[n]$ to recover the pilot signal, $x[n]$. In this section, we provide the mathematical foundations behind each step and describe the procedure for parameter estimation.

The proposed algorithm estimates ε and Ω_d based on a linearized version of the signal model described in Eq. (1). We first estimate ε and use it to compensate $y[n]$. Starting with few samples of the compensated signal, in every subsequent step of the algorithm we provide refined estimates of ε and Ω_d using larger sample sizes. For this, we explore a Taylor series expansion of the imaginary part of the compensated signals. This approximation yields a bias and may not be accurate for large sample batches. The bias originates from the third-order term of the Taylor series expansion and we determine the sample size that minimizes the worst-case MSE and apply a linear estimator.

A. Step 1

Initially, we have no knowledge of ε and assume it to be in the interval $[-\pi, \pi]$. In the worst case, i.e., $\varepsilon = \pm\pi$, this parameter could have a large influence on the subsequent steps of the algorithm, which rely on linearizations. Thus, in the first step of our proposed algorithm, denoted as $k = 1$, we estimate the complex exponential $e^{j\varepsilon}$ and compensate the received signal to reduce the influence of this constant phase term. For this, we average $y[n]$ using N_1 samples and divide by the absolute value of the found average. This is done so that the estimate $(e^{\hat{j}\varepsilon})$ remains on the unit circle. Introducing $P_1 = \lfloor\frac{L-1}{2}\rfloor - \lfloor\frac{N_1-1}{2}\rfloor$ and $P_2 = \lfloor\frac{L-1}{2}\rfloor + \lceil\frac{N_1-1}{2}\rceil$, this procedure is mathematically described by

$$(e^{\hat{j}\varepsilon}) = \frac{\frac{1}{N_1}\sum\limits_{n=P_1}^{P_2} y[n]}{\left|\frac{1}{N_1}\sum\limits_{n=P_1}^{P_2} y[n]\right|}. \qquad (2)$$

We wish to find the number of samples N_1 for which the estimate $(e^{\hat{j}\varepsilon})$ is close to unbiased but still with a relatively low variance. Let us first consider the case where the received signal has no noise. Recall that $x[n]$ is an all-ones vector, the summation in Eq. (2) is written as

$$\sum_{n=P_1}^{P_2} y[n] = e^{j\varepsilon}\left(e^{-j\Omega_d\left(\frac{N_1-1}{2}\right)}\sum_{n=0}^{N_1-1} e^{j\Omega_d n}\right). \qquad (3)$$

The summation term in Eq. (3) can be shown to be

$$\sum_{n=0}^{N_1-1} e^{j\Omega_d n} = \left(\frac{e^{j\Omega_d N_1/2}}{e^{j\Omega_d/2}}\right)\frac{\sin(\Omega_d N_1/2)}{\sin(\Omega_d/2)}. \qquad (4)$$

Inserting Eq. (4) into Eq. (3) and substituting into Eq. (2), we have

$$(e^{\hat{j}\varepsilon}) = e^{j\varepsilon}\left[\frac{\frac{\sin(\Omega_d N_1/2)}{\sin(\Omega_d/2)}}{\left|\frac{\sin(\Omega_d N_1/2)}{\sin(\Omega_d/2)}\right|}\right]. \qquad (5)$$

The factor multiplied with $e^{j\varepsilon}$ in Eq. (5) is always equal to +1 or -1. If it is equal to +1, the estimate $(e^{\hat{j}\varepsilon})$ is unbiased. Otherwise, there is a phase shift and the estimate is biased. For the noiseless case, this phase shift happens for $\Omega_d(N_1/2) = \pm\pi$ (depending on the value of Ω_d). As Ω_d is unknown, we consider the worst-case scenario when no noise is present, i.e., with Ω_W.

The complex-valued noise can make the aforementioned phase shift take place for lower values of N_1. Thus, to avoid this

situation and provide a conservative estimate while retaining a relatively low variance, we take

$$N_1 = \text{round}\left(\frac{1}{2}\left[\frac{2\pi}{\Omega_W}\right]\right). \tag{6}$$

To maintain consistency with the derivations based on Eq. (3), we update $N_1 \leftarrow N_1 + 1$ if N_1 is not even. After calculating $(e^{\hat{j}\varepsilon})$ using Eqs. (2) and (6), we get the final estimate for ε as $\hat{\varepsilon}_1 = \angle(e^{\hat{j}\varepsilon})$ and perform the signal compensation as

$$y_{c,1}[n] = (e^{\hat{j}\varepsilon})^* y[n] = e^{j(\varepsilon - \hat{\varepsilon}_1)} e^{j\Omega_d\left(n - \left(\frac{L-1}{2}\right)\right)} x[n] + w'[n], \tag{7}$$

where $(\cdot)^*$ denotes complex conjugation.

B. Step 2

In step $k = 2$, we estimate $(\varepsilon - \hat{\varepsilon}_1)$ and provide a first estimate for Ω_d. Examining the imaginary part of $y_{c,1}[n]$ and using Euler's identity, we have

$$\text{Im}\{y_{c,1}[n]\} = \sin\left[(\varepsilon - \hat{\varepsilon}_1) + \Omega_d\left(n - \left(\frac{L-1}{2}\right)\right)\right] + \text{Im}\{w'[n]\}. \tag{8}$$

Using the Taylor expansion of a sine function $\sin p = p - p^3/3! + p^5/5! + \dots$, for an arbitrary value p, we truncate Eq. (8) up to the third-order term of this representation,

$$\text{Im}\{y_{c,1}[n]\} = (\varepsilon - \hat{\varepsilon}_1) + \Omega_d\left(n - \left(\frac{L-1}{2}\right)\right) - \frac{1}{6}\left[(\varepsilon - \hat{\varepsilon}_1) + \Omega_d\left(n - \left(\frac{L-1}{2}\right)\right)\right]^3 + \text{Im}\{w'[n]\}. \tag{9}$$

Eq. (9) provides a good approximation provided that $\Omega_d\left(n - \left(\frac{L-1}{2}\right)\right)$ is not too large. As we do not know the parameter Ω_d before the estimation, we consider Eq. (9) to be valid as long as $\Omega_W\left(n - \left(\frac{N_2-1}{2}\right)\right)$ yields an angle smaller than $\pi/3$ for an arbitrary pilot length N_2.

Based on Eq. (9), we denote $a = (\varepsilon - \hat{\varepsilon}_1)$ and $\text{Im}\{\mathbf{y}_{c,1}\} = \text{Im}\{y_{c,1}[n]\}$ for $n = \lfloor\frac{L-1}{2}\rfloor - \lfloor\frac{N_2-1}{2}\rfloor, \dots, \lfloor\frac{L-1}{2}\rfloor + \lceil\frac{N_2-1}{2}\rceil$ to yield the linear model

$$\begin{bmatrix} a \\ \Omega_d \end{bmatrix} = \mathbf{H}\,\text{Im}\{\mathbf{y}_{c,1}\} = \begin{bmatrix} 1 & -\frac{(N_2-1)}{2} \\ 1 & 1 - \frac{(N_2-1)}{2} \\ \vdots & \vdots \\ 1 & \frac{(N_2-1)}{2} \end{bmatrix} \text{Im}\{\mathbf{y}_{c,1}\}. \tag{10}$$

Denoting the estimated parameter vector $\hat{\boldsymbol{\theta}} = \begin{bmatrix} \hat{a} & \hat{\Omega}_d \end{bmatrix}^T$, we can estimate the respective parameters [12, pp. 85, Eq. (4.5)],

$$\hat{\boldsymbol{\theta}} = (\mathbf{H}^T\mathbf{H})^{-1}\mathbf{H}^T\text{Im}\{\mathbf{y}_{c,1}\}. \tag{11}$$

Examining the imaginary part of $y_{c,1}[n]$, the noise power is reduced by half and the covariance matrix of $\hat{\boldsymbol{\theta}}$ is given by $\mathbf{C}_{\hat{\boldsymbol{\theta}}\hat{\boldsymbol{\theta}}} = 0.5\sigma_w^2\left(\mathbf{H}^T\mathbf{H}\right)^{-1}$, which is shown to be [12, pp. 85, Eq. (4.7)]

$$\mathbf{C}_{\hat{\boldsymbol{\theta}}\hat{\boldsymbol{\theta}}} = 0.5\sigma_w^2 \begin{bmatrix} \frac{1}{N_2} & 0 \\ 0 & \frac{12}{N_2(N_2^2-1)} \end{bmatrix}. \tag{12}$$

Clearly, the signal model order given by $\mathbf{H}$ does not match the one in Eq. (9). In fact, the term $-\left[(\varepsilon - \hat{\varepsilon}) + \Omega_d\left(n - \left(\frac{N_2-1}{2}\right)\right)\right]^3/6$ introduces an estimator bias. A large value of N_2 reduces the estimator variance while increasing the bias. Thus, we need to calculate the amount of samples N_2 that gives the best variance/bias trade-off. Since the term $\Omega_d\left(n - \left(\frac{N_2-1}{2}\right)\right)$ dominates over $(\varepsilon - \hat{\varepsilon}_1)$ as n increases, we consider that the bias stems from the factor $-\left[\Omega_d\left(n - \left(\frac{N_2-1}{2}\right)\right)\right]^3/6$.

Expanding Eq. (11), it is possible to demonstrate that, in the absence of noise,

$$\hat{\Omega}_d = \sum_{n=0}^{N_2-1} \text{Im}\{y_{c,1}[n]\}\left(\frac{-6}{N_2^2 + N_2} + \frac{12n}{N_2^3 - N_2}\right)$$
$$= 12\Omega_d\left[\sum_{n=0}^{N_2-1}\left(n - \left(\frac{N_2-1}{2}\right)\right)\frac{n}{N_2^3 - N_2}\right]$$
$$- 2\Omega_d^3\left[\sum_{n=0}^{N_2-1}\left(n - \left(\frac{N_2-1}{2}\right)\right)^3\frac{n}{N_2^3 - N_2}\right]. \tag{13}$$

The second line of Eq. (13) can be shown to be equal to Ω_d, which is the true parameter. The bias therefore comes from the last summation. The bias, represented as $\text{bias}(\Omega_d, N_2)$, can be shown to be

$$\text{bias}(\Omega_d, N_2) = -2\Omega_d^3\left[\sum_{n=0}^{N_2-1}\left(n - \left(\frac{N_2-1}{2}\right)\right)^3\frac{n}{N_2^3 - N_2}\right]$$
$$= \frac{-\Omega_d^3}{15}\left[\frac{(2N_2-1)(3N_2^2 - 3N_2 - 1)}{N_2+1}\right]$$
$$+ \frac{3\Omega_d^3}{4}\left(\frac{N_2(N_2-1)^2}{N_2+1}\right) - \frac{\Omega_d^3}{4}\left(\frac{(N_2-1)^2(2N_2-1)}{N_2+1}\right)$$
$$+ \frac{\Omega_d^3}{8}\left(\frac{(N_2-1)^3}{N_2+1}\right). \tag{14}$$

Recall that all derivations up to this point use a third-order Taylor series expansion of $\text{Im}\{y_{c,1}[n]\}$, assuming it to be a close approximation of the sin function. As a consequence, the bias is expected to be most significant in the last sample of a pilot with length $N_{\max}$. Assuming the third-order Taylor series expansion to be valid up to an angle of $\pi/3$, we use a maximum analyzed pilot length that fulfills

$$\Omega_W\left(\frac{N_{\max}-1}{2}\right) = \frac{\pi}{3}. \tag{15}$$

At the same time, using relatively short pilots to perform the estimation yields a large variance. Consequently, the third-order Taylor series expansion may not provide a good approximation, since $\hat{\Omega}_d(N_{\max} - 1)/2$ can attain a very high value. Hence, we start our analysis with a minimum pilot length $N_{\min}$ that enables such a representation. In our study, given that the noise is Gaussian, the estimated parameters also follow a Gaussian distribution. With the empirical rule that, for this distribution, 95% of the observations fall within two standard deviations from the mean value, we choose $N_{\min}$ based on Eq. (12) such that

$$2\sqrt{\frac{6\sigma_w^2}{N_{\min}^3 - N_{\min}}} = \frac{\Omega_W}{2}. \tag{16}$$

The criterion we use to choose $N_2 \in [N_{\min}, N_{\max}]$ for application in Eq. (11) is the MSE in the last sample, given for $n = N_{\max} - 1$, as the bias is expected to be more pronounced. Again, since we do not have prior knowledge of Ω_d, we use Ω_W to provide a worst-case MSE. Using Eqs. (12) and (14), it is possible to show that [12, pp. 19, Eq. (2.6)]

$$\text{MSE}_{\text{worst-case}} = \frac{\sigma_w^2}{2N_2} + \frac{6\sigma_w^2}{N_2(N_2^2 - 1)} \left(\frac{N_{\max} - 1}{2} \right)^2$$
$$+ \text{bias}^2(\Omega_W, N_2) \left(\frac{N_{\max} - 1}{2} \right)^2 + \frac{\sigma_w^2}{2}. \quad (17)$$

We choose the value of N_2 that minimizes the MSE in Eq. (17). This can be done, e.g., by line search. If N_2 is odd, we take $N_2 \leftarrow N_2 + 1$ to preserve the diagonality of $\mathbf{C}_{\hat{\theta}\hat{\theta}}$.

Following, we apply Eq. (11) and update the estimates. Their final values are $\hat{\varepsilon}_2 = \hat{\varepsilon}_1 + \hat{a}$ and $\hat{\Omega}_{d,2} = \hat{\Omega}_d$. Finally, the compensated signal after step 2 for $n = 0, \ldots, L - 1$ is

$$y_{c,2}[n] = e^{-j\hat{\varepsilon}_2} e^{-j\hat{\Omega}_{d,2}\left(n - \left(\frac{L-1}{2}\right)\right)} y[n]$$
$$= e^{j(\varepsilon - \hat{\varepsilon}_2)} e^{j(\Omega_d - \hat{\Omega}_{d,2})\left(n - \left(\frac{L-1}{2}\right)\right)} x[n] + w'[n]. \quad (18)$$

C. Step 3 and beyond

In steps $k \geq 3$, the error from the previous iterations is estimated and used to improve the final estimates. Introducing $a = (\varepsilon - \hat{\varepsilon}_{k-1})$ and $b = (\Omega_d - \hat{\Omega}_{d,k-1})$, the compensated signal calculated using the most recent available estimates is represented as $y_{c,k-1}[n] = e^{-j\hat{\varepsilon}_{k-1}} e^{-j\hat{\Omega}_{d,k-1}\left(n - \left(\frac{L-1}{2}\right)\right)} y[n]$. The signal model from Eq. (10) is used to write

$$\begin{bmatrix} a \\ b \end{bmatrix} = \mathbf{H} \, \text{Im}\{\mathbf{y}_{c,k-1}\} = \begin{bmatrix} 1 & -\frac{(N_k - 1)}{2} \\ 1 & 1 - \frac{(N_k - 1)}{2} \\ \vdots & \vdots \\ 1 & \frac{(N_k - 1)}{2} \end{bmatrix} \text{Im}\{\mathbf{y}_{c,k-1}\}. \quad (19)$$

In Eq. (19), $\text{Im}\{\mathbf{y}_{c,k-1}\} = \text{Im}\{y_{c,k-1}[n]\}$ for the indices $n = \lfloor \frac{L-1}{2} \rfloor - \lfloor \frac{N_k - 1}{2} \rfloor, \ldots, \lfloor \frac{L-1}{2} \rfloor + \lceil \frac{N_k - 1}{2} \rceil$. As in Sec. III-B, we wish to find a pilot length N_k that minimizes the worst-case MSE for use with the estimator as in Eq. (11), $\text{Im}\{\mathbf{y}_{c,k-1}\}$ and $\hat{\boldsymbol{\theta}} = \begin{bmatrix} \hat{a} & \hat{b} \end{bmatrix}^T$. Proceeding as in Step 2 of the algorithm, now assuming that the estimates in the previous iteration are located according to the mentioned empirical rule in Section III-B, we can apply Eqs. (14) and (17) as a function of N_k, utilizing $2\sqrt{\frac{6\sigma_w^2}{N_{k-1}^3 - N_{k-1}}}$ instead of Ω_W. $N_{\max}$ and $N_{\min}$ are given by

$$2\sqrt{\frac{6\sigma_w^2}{N_{k-1}^3 - N_{k-1}}} \left(\frac{N_{\max} - 1}{2} \right) = \frac{\pi}{3}, \quad (20)$$

$$2\sqrt{\frac{6\sigma_w^2}{N_{\min}^3 - N_{\min}}} = \sqrt{\frac{6\sigma_w^2}{N_{k-1}^3 - N_{k-1}}}. \quad (21)$$

The final estimates are $\hat{\varepsilon}_k = \hat{\varepsilon}_{k-1} + \hat{a}$ and $\hat{\Omega}_{d,k} = \hat{\Omega}_{d,k-1} + \hat{b}$. The estimation procedure runs until a defined stop criterion is met. This can for example be when $|\hat{b}| \leq \delta$ for some δ. In addition, if at any step of the algorithm we find $N_{\min}, N_k$ or $N_{\max} > L$,

we can set them to L respectively. As in the previous steps, if N_k is odd, we take $N_k \leftarrow N_k + 1$.

For any iteration k, we write the compensated signal as

$$y_{c,k}[n] = e^{-j\hat{\varepsilon}_k} e^{-j\hat{\Omega}_{d,k}\left(n - \left(\frac{L-1}{2}\right)\right)} y[n]$$
$$= e^{j(\varepsilon - \hat{\varepsilon}_k)} e^{j(\Omega_d - \hat{\Omega}_{d,k})\left(n - \left(\frac{L-1}{2}\right)\right)} x[n] + w'[n]. \quad (22)$$

Algorithm 1 Estimation procedure

    Inputs: Ω_W, all-ones vector $x[n]$ with even length L, observations $y[n]$, σ_w^2, δ
    Outputs: $\hat{\varepsilon}$, $\hat{\Omega}_d$
1: $k = 1$ ▷ Start of step 1
2: Calculate N_1 (Eq. (6))
3: $N_1 \leftarrow \min(N_1, L)$
4: $N_1 \leftarrow N_1 + \mod(N_1, 2)$
5: Calculate $\hat{\varepsilon}_1 = \angle(e^{\hat{j}\varepsilon})$ (Eq. (2))
6: Calculate $y_{c,1}[n]$ (Eq. (7))   ▷ End of step 1
7: $k \leftarrow k + 1$ ▷ Start of step 2
8: Calculate $N_{\min}$ (Eq. (16)) and $N_{\max}$ (Eq. (15))
9: $N_{\min} \leftarrow \min(N_{\min}, L)$, $N_{\max} \leftarrow \min(N_{\max}, L)$
10: $N_2 = \text{argmin MSE}_{\text{worst-case}}$ (Eq. (17)) using bias(Ω_W, N_2)
11: $N_2 \leftarrow N_2 + \mod(N_2, 2)$
12: Calculate $\hat{a}$ and $\hat{\Omega}_d$ (Eq. (11))
13: Update $\hat{\varepsilon}_2 \leftarrow \hat{\varepsilon}_1 + \hat{a}$ and $\hat{\Omega}_{d,2} \leftarrow \hat{\Omega}_d$
14: Calculate $y_{c,2}[n]$ (Eq. (18))   ▷ End of step 2
15: **while** $|\hat{b}| < \delta$ **do**
16:      $k \leftarrow k + 1$ ▷ Start of step k
17:      Calculate $N_{\min}$ (Eq. (21)) and $N_{\max}$ (Eq. (20))
18:      $N_{\min} \leftarrow \min(N_{\min}, L)$, $N_{\max} \leftarrow \min(N_{\max}, L)$
19:      $N_k = \text{argmin MSE}_{\text{worst-case}}$ (Eq. (17)) using bias $\left(2\sqrt{\frac{6\sigma_w^2}{N_{k-1}^3 - N_{k-1}}}, N_k \right)$
20:      $N_k \leftarrow N_k + \mod(N_k, 2)$
21:      Calculate $\hat{a}$ and $\hat{b}$ (Eq. (11)) using $\text{Im}\{\mathbf{y}_{c,k-1}\}$
22:      Update $\hat{\varepsilon}_k \leftarrow \hat{\varepsilon}_{k-1} + \hat{a}$ and $\hat{\Omega}_{d,k} \leftarrow \hat{\Omega}_{d,k-1} + \hat{b}$
23:      Calculate $y_{c,k}[n]$ (Eq. (22))   ▷ End of step k
24: **end while**

IV. SIMULATION RESULTS

The performance of the proposed algorithm is evaluated in terms of estimator bias and variance at SNR $= [-10, 15]$ dB using 10^5 realizations for each SNR value. The system parameters are listed in Tab. I.

TABLE I
SYSTEM SIMULATION VARIABLES

Variable	Value	Variable	Value	Variable	Value
f_c	75GHz	L	500	Ω_d	0.027071
v	7km/s	α	$10°$	Ω_W	0.027489
f_s	400MHz	ε	1.2	δ	10^{-14}

The CRLB for each parameter is found directly in Eq. (12), since $\mathbf{C}_{\hat{\theta}\hat{\theta}}$ is diagonal. First, the variance of the estimates using our proposed method is shown in Fig. 2, together with
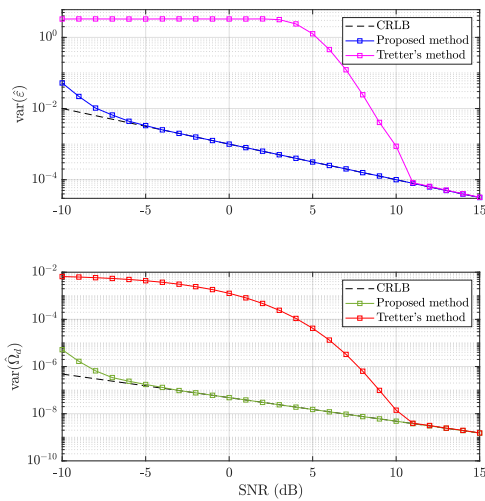
Fig. 2. Estimator variances for $\hat{\varepsilon}$ and $\hat{\Omega}_d$ and their associated CRLBs.
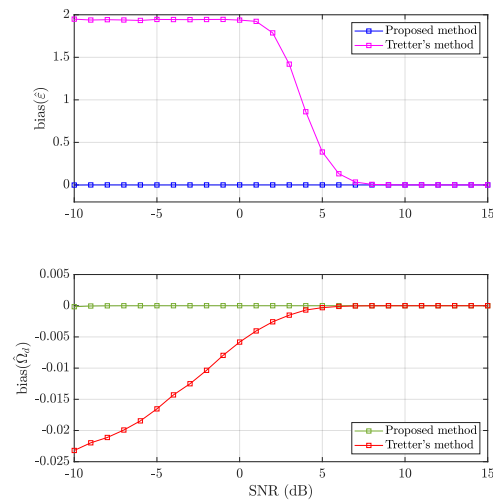
Fig. 3. Estimator biases for $\hat{\varepsilon}$ and $\hat{\Omega}_d$.

the estimator variance using Tretter's method, which assumes a signal model similar to that of Eq. (1) and has a simple implementation. Observe that the estimator variances of the proposed algorithm are very close to the respective CRLBs, even at low SNRs. The variances start to deviate significantly from the CRLBs at SNR $= -6$dB. In contrast, using Tretter's method, the respective variances considerably diverge from the CRLB already at 10dB, highlighting the difference in performance between the compared approaches. The estimator biases from each method are shown in Fig. 3.

For the simulated SNR range, the strongest biases for $\hat{\varepsilon}$ and $\hat{\Omega}_d$ using our proposed method are, respectively, -1.29×10^{-3} and -1.58×10^{-4}, which gives a pronounced difference. However, the errors in the estimation for ε are not as significant, since this parameter does not strongly contribute to the worst-case error, i.e., at $n = L - 1$. The errors in the estimation for Ω_d are more relevant, as this parameter scales with n.

The achieved bias using Tretter's method for $\hat{\varepsilon}$ and $\hat{\Omega}_d$ is relatively relevant at SNR levels of 7dB and 5dB respectively, showing the limited performance of this approach. An explanation for such degradation is the fact that Tretter's method applies phase unwrapping, which is difficult at low SNR regimes [13].

V. CONCLUSIONS AND FUTURE WORK

In this paper, a simple signal model was used to estimate Doppler shifts in satellite communications. Based on a linearization of this model, a multi-step algorithm to estimate a constant phase term and a normalized Doppler shift based on linear estimators was developed. The estimation procedure shows close to unbiased estimates with variances approaching the CRLB for a broad range of SNR regimes, performing better than the well-known Tretter's method. This shows the potential of the proposed algorithm in problems based on the respective signal model. Furthermore, as a standalone procedure, the proposed algorithm does not depend on other subsystems, such as the global navigation satellite system, to estimate Doppler shifts.

REFERENCES

[1] G. Araniti, A. Iera, S. Pizzi, and F. Rinaldi, "Toward 6G non-terrestrial networks," *IEEE Network*, vol. 36, no. 1, pp. 113–120, 2022.

[2] B. Zong *et al.*, "6G technologies: key drivers, core requirements, system architectures, and enabling technologies," *IEEE Vehicular Technology Magazine*, vol. 14, no. 3, pp. 18–27, 2019.

[3] A. Vanelli-Coralli, A. Guidotti, T. Foggi, G. Colavolpe, and G. Montorsi, "5G and beyond 5G non-terrestrial networks: trends and research challenges," in *IEEE 3rd 5G World Forum (5GWF)*, 2020, pp. 163–169.

[4] M. Huang, J. Chen, and S. Feng, "Synchronization for OFDM-based satellite communication system," *IEEE Transactions on Vehicular Technology*, vol. 70, no. 6, pp. 5693–5702, 2021.

[5] Z. Shujuan, L. Xiaofeng, and J. Min, "A frequency synchronization algorithm for OFDM in mobile satellite communication systems," in *IEEE Conference Anthology*, 2013, pp. 1–4.

[6] W. Wang *et al.*, "Near optimal timing and frequency offset estimation for 5G integrated LEO satellite communication system," *IEEE Access*, vol. 7, pp. 113 298–113 310, 2019.

[7] J. Wang, C. Jiang, L. Kuang, and B. Yang, "Iterative Doppler frequency offset estimation in satellite high-mobility communications," *IEEE Journal on Selected Areas in Communications*, vol. 38, no. 12, pp. 2875–2888, 2020.

[8] S. Li *et al.*, "Downlink carrier frequency offset estimation for OTFS-based LEO satellite communication system," *IEEE Communications Letters*, vol. 28, no. 1, pp. 163–167, 2024.

[9] R. Hadani *et al.*, "Orthogonal Time Frequency Space Modulation," in *IEEE Wireless Communications and Networking Conference (WCNC)*, 2017, pp. 1–6.

[10] M. Bayat and A. Farhang, "Time and frequency synchronization for OTFS," *IEEE Wireless Communications Letters*, vol. 11, no. 12, pp. 2670–2674, 2022.

[11] S. Tretter, "Estimating the frequency of a noisy sinusoid by linear regression," *IEEE Transactions on Information Theory*, vol. 31, no. 6, pp. 832–835, 1985.

[12] S. M. Kay, *Fundamentals of Statistical Signal Processing: Estimation Theory*. Prentice-Hall, 1993.

[13] S. Kay, "A fast and accurate single frequency estimator," *IEEE Transactions on Acoustics, Speech, and Signal Processing*, vol. 37, no. 12, pp. 1987–1990, 1989.